1-1-2018

Alkaline Fuel Cells with Novel Gortex-Based Electrodes are Powered Remarkably Efficiently by Methane Containing 5% Hydrogen

Klaudia K. Wagner
University of Wollongong, kwagner@uow.edu.au

Prerna Tiwari
University of Wollongong, pt832@uowmail.edu.au

Gerhard F. Swiegers
University of Wollongong, swiegers@uow.edu.au

Gordon G. Wallace
University of Wollongong, gwallace@uow.edu.au

Alkaline Fuel Cells with Novel Gortex-Based Electrodes are Powered Remarkably Efficiently by Methane Containing 5% Hydrogen

Abstract

Numerous electric and gas utilities are actively pursuing "power-to-gas" technology, which involves using unwanted, excess renewable energy to manufacture hydrogen gas (H 2) that is then injected into the existing natural gas pipeline network in 5-10% by volume. This work reports an alkaline fuel cell that has the potential to harness such gas mixtures for downstream generation of electric power. The fuel cell, which employs novel Gortex-based electrodes layered with Pd/Pt catalysts, generates electricity remarkably efficiently when fuelled with methane (CH 4) containing 5% hydrogen. Methane constitutes the major component of natural gas. The fuel cell has been studied over a range of hydrogen to methane ratios using Tafel plots and electrochemical impedance spectroscopy. These show that, in terms of fundamental operation, there is, astonishingly, almost no difference between using pure hydrogen and 5% hydrogen in methane, as the fuel. The Gortex electrodes and alkaline electrolyte are clearly able to utilize the dilute hydrogen as a fuel with remarkable efficiency. The methane acts as an inert carrier gas and is not consumed.

Disciplines

Engineering | Physical Sciences and Mathematics

Publication Details

Wagner, K., Tiwari, P., Swiegers, G. F. & Wallace, G. G. (2018). Alkaline Fuel Cells with Novel Gortex-Based Electrodes are Powered Remarkably Efficiently by Methane Containing 5% Hydrogen. Advanced Energy Materials, 8 (7), 1702285-1-1702285-10.

Alkaline Fuel Cells with Novel Gortex-based Electrodes are Powered Remarkably Efficiently by Methane Containing 5% Hydrogen

Klaudia Wagner,*[a] Prerna Tiwari,[a] Gerhard F. Swiegers*[a] and Gordon G. Wallace[a]

Numerous electric and gas utilities are actively pursuing *"Power-to-Gas"* (P2G) technology, which involves using unwanted, excess renewable energy to manufacture hydrogen gas (H_2) that is then injected into the existing natural gas pipeline network in 5-10% by volume. This work reports an alkaline fuel cell that has the potential to harness such gas mixtures for downstream generation of electric power. The fuel cell, which employs novel Gortex-based electrodes layered with Pd/Pt catalysts, generates electricity remarkably efficiently when fuelled with methane (CH_4) containing 5% hydrogen. Methane constitutes the major component of natural gas. The fuel cell has been studied over a range of hydrogen to methane ratios using Tafel plots and electrochemical impedance spectroscopy. These show that, in terms of fundamental operation, there is, astonishingly, almost no difference between using pure hydrogen and 5% hydrogen in methane, as the fuel. The Gortex electrodes and alkaline electrolyte are clearly able to utilize the dilute hydrogen as a fuel with remarkable efficiency. The methane acts as an inert carrier gas and is not consumed.

1. Introduction

Blending hydrogen (H_2) manufactured from excess renewable energy into the existing natural gas pipeline network forms the basis of so-called "*Power-to-Gas*" (P2G) technology (Figure 1(a)).[1] P2G is presently being actively pursued by many electrical and gas utilities. Not only does P2G allow for an increased deployment of renewable energy sources (like biomass, solar or wind) on electrical grids, it also helps balance the grid and monetizes renewable energy that is generated at times of low electrical demand. The natural gas network has a vast potential for hydrogen storage.[1] It has also been proposed as a means of transporting hydrogen to downstream, end-user markets.[1(a)] As a practical outcome of P2G, it is anticipated that many future natural gas networks will routinely contain a proportion of hydrogen.[1] This is likely to be less than 10% by volume as this is the maximum that natural gas pipelines can accommodate without downstream engineering modifications.[1] Natural gas is primarily composed of methane (CH_4), but also contains quantities of ethane, propane and heavier hydrocarbons.[1]

If the hydrogen-enriched natural gas streams of P2G could be used to generate electricity, then this would provide additional economic benefits. A hydrogen-oxygen fuel cell capable of doing so would, however, need to be successfully and sustainably fueled by the low levels of hydrogen present. That is, the fuel cell would have to be capable of utilizing the <10% hydrogen blend as a fuel. The most widely used class of hydrogen-oxygen fuel cell at present is the Proton Exchange Membrane (PEM) fuel cell. Studies have demonstrated that methane acts an inert gas when fed through the anode of a PEM.[2(a),(b)] PEM fuel cells have, moreover, been shown to be capable of generating electrical power when fueled with a blend of 5% hydrogen in nitrogen (N_2),[2(c)] which also acts as an inert gas in such cells. However, at such high dilutions, PEM fuel cells are known to experience significant resistances arising from proton diffusion limitations due to the solid-state PEM electrolyte

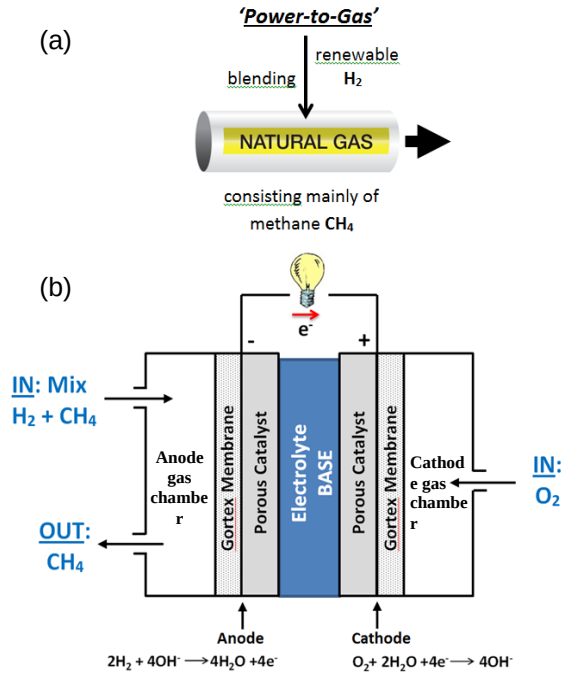

Figure 1. (a) Principle of "*Power-to-Gas*", in which hydrogen manufactured from excess renewable energy, is injected in existing natural gas pipelines. Natural gas is mainly methane. (b) Schematic diagram of the fuel cell of the present study.

[a] *Dr Klaudia Wagner, Ms Prerna Tiwari, Prof Dr Gerhard F. Swiegers and Prof Dr Gordon G. Wallace*
Intelligent Polymer Research Institute and ARC Centre of Excellence for Electromaterials Science
University of Wollongong, Wollongong, NSW 2522 (Australia)
Corresponding author e-mail: Swiegers@uow.edu.au

and its interface with the solid catalysts.[2(d)] Thus, for example, the charge transfer resistance in a PEM fuel cell increased from 330 mΩ cm^2 when fueled with pure hydrogen, to 780 mΩ cm^2 when the hydrogen was diluted to 5% by volume with nitrogen - a 240% increase (all feedstock gases humidified to 91%).[2(c)] It is perhaps for this reason that PEM fuel cells capable of operating with 5-10% hydrogen in methane do not appear to have ever been proposed or studied.

Another reason may involve the need to humidify feedstock gases in PEM fuel cells in order to maintain the conductivity of the proton exchange membrane. Natural gas transported by pipeline is routinely extremely dry.[1] If a PEM fuel cell were used to extract electricity from hydrogen-enriched natural gas, then the gas would first have to be humidified before entering the cell. It may then also have to be de-humidified after leaving the cell and before re-entering the natural gas pipeline.

An alternative class of hydrogen-oxygen fuel cell is the alkaline fuel cell (AFC). AFCs were one of the first fuel cell technologies applied to practical power generation, with applications in space, including the Apollo missions and the Space Shuttle.[3,4] Their limited application outside of space missions arose mostly because of a key disadvantage of the alkaline electrolytes used, namely, carbon dioxide (CO_2) poisoning.[5,6] This problem led to an almost complete termination of activities in alkaline fuel cell research in the early 1990s.[7] However, the CO_2 tolerance of more modern AFC gas diffusion electrodes has overcome this problem and, as the alkaline electrolyte is easily exchanged, it seems that CO_2 in the air is no longer a major problem for AFCs.[8] Given their simplicity of operation and low cost, AFCs are being reconsidered for commercialization.[9]

AFCs normally employ liquid alkaline electrolytes (typically 6 M KOH), which provides faster reaction kinetics and allows the use of non-noble metals like Ni or Ag as catalysts.[10] All AFCs employ gas-diffusion electrodes, within which a high interfacial contact area is needed between three phases: solid (electrode), liquid (electrolyte), and gas (reactant).[4] Hydrogen is fed into the anode, where it is oxidized and combined with hydroxide ions (OH^-) to form water. The hydrogen oxidation reaction (HOR) that occurs on the anode is shown in eq. 1:

$$2\ H_2 + 4\ OH^- \rightarrow 4\ H_2O + 4\ e^- \qquad \text{(eq. 1)}$$

The electrons generated at the anode flow to the cathode, where the oxygen reduction reaction (ORR) takes place (eq. 2):

$$O_2 + 2\ H_2O + 4\ e^- \rightarrow 4\ OH^- \qquad \text{(eq. 2)}$$

The OH^- ions produced at the cathode diffuse through the electrolyte to the anode, to thereby close the cycle.[11]

In this study we report that alkaline fuel cells containing two porous, Gortex-based gas diffusion electrodes[12,13] layered with Pd/Pt catalysts, binders, and a current carrying Ni mesh, are capable of remarkably efficiently utilising even extremely dilute hydrogen-methane mixtures as fuels (Figure 1(b)). Mixtures containing as little as 5% hydrogen by volume may be used without an apparent energy penalty. Fuel cells of this type have the potential to harness the dilute gas mixtures of *Power-to-Gas* for the local generation of electrical power.

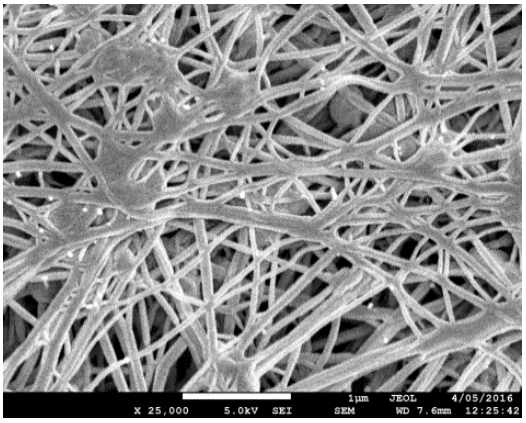

(a)

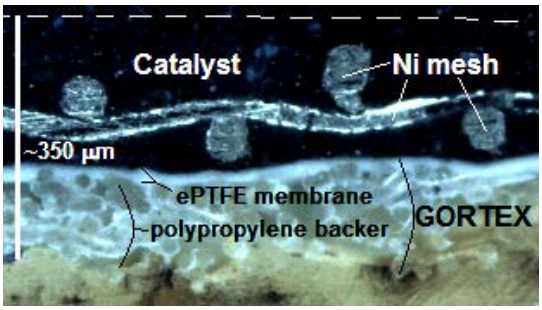

(b)

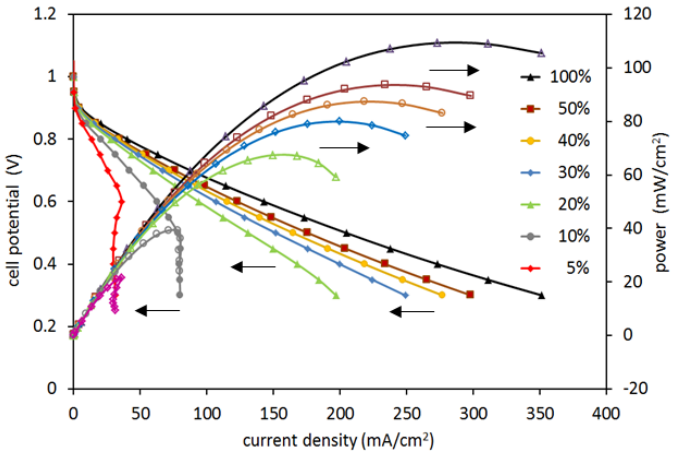

(c)

Figure 2. (a) Scanning electron microscopy image of the Gortex substrate used to fabricate the electrodes of this study; (b) cross-section of the electrodes, showing the Gortex membrane with polypropylene backer at the bottom and the Ni mesh and catalyst at the top. The dashed line at the top of the image depicts the surface of the catalyst layer; (c) Typical fuel cell voltage-current density characteristic, (j-V) and (d) the (j-V) and power density–current density (j-P) curves for a fuel cell operating between 5% and 100% of hydrogen in a gas mixture.

2. Results and Discussion

2.1 The Use of *Expanded PTFE* (*ePTFE*) Membranes ('*Gortex'*) as Electrode Substrates

Also known as *expanded PTFE* (or *ePTFE)*, Gortex consists of a porous bed of microscopically-small Teflon filaments that are individually and collectively highly hydrophobic (Figure 2(a)).[14] *ePTFE* has been employed in innumerable applications since its discovery in the 1960's, including, most prominently, as a water-resistant textile.[15] Other applications have included: as a sealant, filter, coating, and in medical devices.[15] The classic feature of *Gortex* is that water vapour (and gases in general) readily passes through it, but not liquid water. This is a consequence of its high porosity (e.g. 80%), combined with its high hydrophobicity. Thus, when worn as a textile, Gortex allows water vapour from a wearer's body to pass through it, but not liquid water from rain.

While certain air electrodes have long utilized Gortex as an outmost "water-exclusion" layer, it has only recently been examined as an electrode substrate in its own right.[12,13] One important feature of Gortex in this respect is that it has a pore structure that is far more uniform and hydrophobic than present gas diffusion electrodes. When used as a substrate for a gas diffusion electrode, finely-pored Gortex may therefore impart an unprecedented resistance to flooding by aqueous electrolytes. We have recently reported Gortex-based electrodes that flood only when the overpressure on the water-side is >4 bar,[12(a)] which is an order of magnitude greater than most conventional gas diffusion electrodes (typically <0.1 bar)[16] and, as far as we are aware, better than the best GDE yet reported (0.2 bar).[17] The phenomenon of flooding has, to date, effectively blocked the widespread use of gas diffusion electrodes in industrial electrochemistry. Several industrial electrochemical processes, including the chlor-alkali process,[16] could be drastically improved by introducing (via a gas diffusion electrode), a "de-polarising" gas (e.g. air oxygen) to their otherwise unproductive counter electrodes.[16] The chlor-alkali process reputedly consumes ca. 2% of the USA's electricity production.[16] Gortex electrodes coated with conducting polymer catalysts have also been studied in fuel cells and electrolysers.[12,13]

In this work we report the fabrication and study of an alkaline fuel cell containing two Gortex-based gas diffusion electrodes, as depicted schematically in Figure 1(b). Figure 2(a) provides a scanning electron microscope (SEM) image of the Gortex substrate, which was a General Electric Energy *Preveil*^{TM} expanded PTFE (ePTFE) membrane (20 μm thick), backed with a polypropylene lattice. Each Gortex substrate was coated with a porous, conductive catalyst layer comprising 20% Pd-Pt, carbon black (CB), incorporating dispersed poly (tetrafluoroethylene) (PTFE) binder, and a current carrier Ni mesh (as described in the Experimental Section). Figure 2(b) is a photographic cross-section of the electrodes, showing the Gortex substrate with polypropylene backer at the bottom (gas side of the gas diffusion electrode), and the Ni mesh and catalyst/carbon black at the top (aqueous electrolyte side of the gas diffusion electrode). The electrodes were unique in that they did not flood until the overpressure on the aqueous electrolyte side exceeded 4 bar.[12(a)]

Table 1. Parameters of the flow of H_2 and CH_4 in examined mixtures, and obtained: open circuit voltage (Voc), potential upon applying current density of 10 mA/cm^2 (E), the highest power density (P_{max}) and ohmic resistance (R_{slop_unc}) from uncorrected polarization curves.

H_2 %	H_2 ml/min	CH_4 ml/min	Voc V	E at 10 mA/cm^2 V	P_{max} mW/cm^2	R_{slop_unc}
100	10	0	1.03	0.88	109.3	1.5
50	10	10	1.03	0.88	93.4	1.8
40	8	12	1.03	0.88	87.4	1.9
30	6	14	1.02	0.87	79.9	2.1
20	4	16	1.01	0.87	67.4	2.8
10	2	18	1.00	0.85	39.2	4.9
5	1	19	0.99	0.82	21.6	7.8
100[a]	10	0	1.04	0.89	96.7	1.8

[a] after methane exposure

2.2 Fuel Cell Operation using Methane Blends Containing 5%-100% Hydrogen

During the experiments, pure hydrogen or mixtures of hydrogen and methane, at atmospheric pressure, were allowed to slowly flow through the anode gas chamber of the test cell while oxygen gas at atmospheric pressure was slowly passed through the cathode gas chamber (Figure 1(b)). Each of the gases were employed in high purity form. The liquid electrolyte in the cell was 6 M KOH. The cell was designed to ensure that each Gortex-based gas diffusion electrode had a 1 cm^2 geometric area. The anode and cathode electrodes were located in a facing disposition to each other and separated by an inter-electrode gap of 3 mm. No diaphragm, ionomer, or other separator was required in the gap between the electrodes in the cell.

The performance of the above-described alkaline fuel cell was initially examined with mixtures of hydrogen in methane of: 50%, 40%, 30%, 20%, 10% and 5%. The total flow of the H_2-CH_4 mixture in these experiments was kept constant at 20 ml/min. Detailed flow conditions are summarised in Table 1. Comparative experiments using pure hydrogen, were performed before and after the experiments with the hydrogen-methane mixtures, in order to assess the stability of the system to changes in the dilution.

A voltage drop of only 40 mV in the open circuit potential (Voc) was observed when cells were supplied with pure hydrogen compared with cells supplied with a methane blend containing 5% hydrogen. A 60 mV voltage drop was seen at a low current density of 10 mA/cm^2 (Table 1).

2.3 Polarisation Curves

To characterize the overall fuel cell performance, polarization curves were measured. These curves plot voltage against current. Curves of this type have three different regions: (i) *a kinetic*, (ii) *an ohmic*, and (iii) a *mass transport* region. The kinetic region (non-linear voltage drop at the low current density),

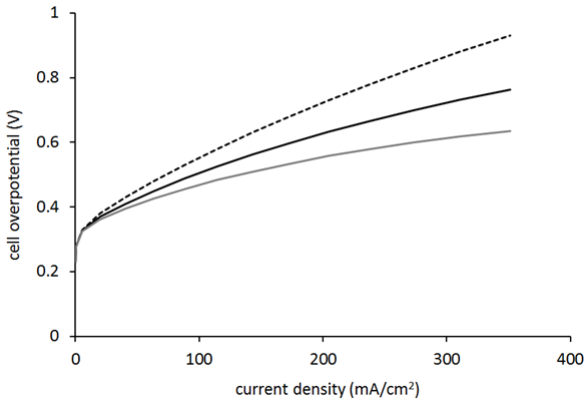

Figure 3. Polarization curves for pure hydrogen, uncorrected data (dash line), corrected by: (i) taking into account the electrolyte resistance (black line) and (ii) using EIS (grey line)).

relates to the proportion of energy needed to start the chemical reactions on both electrodes. In this region, activation losses dominate the cell behaviour. In the ohmic region, kinetic, ohmic, and mass transport losses all participate, but ohmic losses dominate, and yield a linear polarization curve. Finally, in the *mass transport* region, losses derive from an insufficient supply of reactant/s, causing a significant nonlinearity.[18,19]

Figure 2(c) displays the polarization curves (filled markers), and power curves (empty markers) of the gas mixtures investigated. Cell potentials were measured between the cathode and anode, meaning that the polarization curves represent the combination of the polarizations of these two electrodes.

For the gas mixtures above, the linear part of the polarization curves demonstrated a gradual increase in slope with declining hydrogen proportions, from 1.5 Ω for pure hydrogen to 7.8 Ω for 5% H_2. This indicates a concomitantly increasing resistance according to Ohm's law (eq. 3):

$$U = iR \qquad \text{(eq. 3)}$$

where i is the current flowing through the cell, and R is the total cell resistance, which includes electronic, ionic, and contact resistance.

The estimated resistances from uncorrected polarization slopes (R_{slop_unc}) for all gases are given in the final column on the right in Table 1.

The mass transport limitations in the polarization curves are obvious for the 5% and 10% hydrogen mixtures, with discontinuities occurring at 0.5 V for the 10% mixture and at 0.6 V for the 5% mixture (Figure 2(c)). At the latter discontinuity at 0.6 V, the hydrogen in the 5% mixture clearly became almost depleted, with a noticeably impairment to the performance of the cell. The losses due to concentration occur over the entire range of current densities, but become more prominent at higher current densities, where the reaction rates are higher, causing faster consumption of reactants. A concentration gradient was formed if mass transport was not fast enough to supply the hydrogen fuel from the bulk of the gas mixture into the anode interface, causing the potential loss. Several processes may contribute to this, such as slow diffusion in the gas phase of hydrogen into the electrode pores, solution/dissolution of reactants/products into/out of the electrolyte, or diffusion of reactants/products through the electrolyte to/from the electrochemical reaction site.

It can be seen that the percentage of hydrogen in the mixture had an impact on the maximum power density. With pure hydrogen the highest power density was 109.3 mW/cm^2. Dilution of the hydrogen decreased the maximum power density to 21.6 mW/cm^2 at 5% hydrogen in mixture (Table 1).

To extract information about the kinetic and mass transport losses as well as the ohmic resistance of the cell, the cell overpotential using pure hydrogen, was plotted as a function of current density (Figure 3).

The ohmic resistance of the supporting electrolyte (E_{el}) depends on the anode-to-cathode spacing or the charge-transport length (d), the cross-sectional area of charge transport (A) and the ionic conductivity (σ) (eq. 4)

$$E_{el} = \frac{d}{\sigma A} \qquad \text{(eq. 4)}$$

The E_{el} of the 6 M KOH electrolyte was calculated for 0.48 Ω (d = 0.3 cm, σ = 0.63 S/cm,[20] and A = 1 cm^2). Polarization curves were then IR-corrected by adding the current multiplied by the electrolyte resistance. Figure 3 shows the uncorrected polarization curve for pure hydrogen (Figure 3; dashed line) and the same curve corrected for the solution resistance (Figure 3; black line). The slope was still significant however.

To better isolate the kinetic losses, the ohmic resistance (R_0=0.90±0.01) from electrochemical impedance spectroscopy (EIS) was applied to the correction in the same fashion (Figure 3; grey line). Impedance-corrected polarization curves were later also used for the generation of the Tafel plots.

2.4 Tafel Plots

At low current densities, electrochemical kinetics are commonly modelled by the Tafel equation, given in eq. 5.

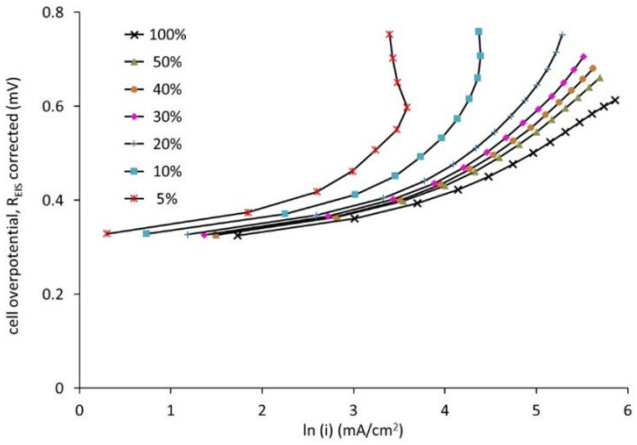

Figure 4. Tafel plots for the fuel cell fuelled with mixtures of between 5% and 100% hydrogen in methane.

$$\eta = A\ln\left(\frac{i}{i_o}\right) \qquad \text{(eq. 5)}$$

where η defines the overpotential, which is the difference between the electrode potential E and the standard potential E_0 ($\eta = E - E_0$), i denotes the current density, i_o is the exchange current density, and A is the Tafel slope. The Tafel slope provides insight into the reaction kinetics and also the mechanism, to thereby elucidate the elementary steps and the rate determining steps. A is higher for an electrochemical reaction that is slow, since slow reaction leads to a higher overvoltage and the exchange current density i_o can be considered to be the current density at which the overvoltage begins to move from zero. If i_o is high, then the surface of the electrode is more 'active' and a current in one particular direction is more likely to flow. It is desired to have as high a value of i_o as possible, and as rapid kinetics as possible (low A).

Figure 4 provides impedance-corrected Tafel plots for all gas mixtures investigated. Table 2 gives slopes (A) (in units of mV/dec) and exchange current densities (i_o) (in units of mA/mg_{cat}) calculated from the catalyst loading.

The estimated Tafel slope for pure hydrogen was 124 mV/dec. This is consistent with the reported literature, Tafel slopes of ca. 120 mV/ dec and higher are frequently reported for both the hydrogen oxidation reaction (HOR) and the oxygen reduction reaction (ORR) in alkaline medium, and on Pt/C.[21,22]

The slopes for all hydrogen-methane mixtures are higher in comparison to pure hydrogen and vary between 155-190 mV/dec, which suggest slower kinetics.

The exchange current density i_o estimated from the Tafel plots were higher for the mixtures with 20-50% hydrogen and lower for 10% and 5% compared to the i_o of pure hydrogen (Table 2). The reasons for this increase are not clear, however as noted by Almutairi and colleagues,[23] the Gibbs free energy ($\Delta G°$) and standard equilibrium voltage (E^0) in eq. 6, considered as the Voc, are higher for methane than for hydrogen. This was used by these authors to explain the higher voltages observed with the addition of methane into hydrogen.

$$E^0 = -\frac{\Delta G^0}{zF} \qquad \text{(eq. 6)}$$

(Methane: $\Delta G°$= –818 kJ/mol, $E°$= 1.41 V versus hydrogen: $\Delta G°$= –237 kJ/mol, $E°$=1.23 V, z is the molar number of electrons transferred and F is the Faraday constant)

The lower i_o for the 5-10% gas mixtures can possibly be explained by the reduced access of hydrogen to the three-way solid-liquid-gas interface in the Gortex-based electrode, while competing with the methane flow. However, as can be seen in Figure 4, the Tafel plots are strongly influenced by concentration losses in these diluted mixtures, and as recognised by Shinagawa and co-workers,[22] the contribution of mass-transport can lead to misinterpretation of the kinetics due to inaccurate Tafel slopes.

Perhaps the key insight that can be derived from the i_o and A values in Table 2 is the fact that, despite the differences, they are all of similar order. This is, in fact, rather stunning given the enormous differences in the proportion of hydrogen present in the mixtures fed into the cells. It indicates that all of the fuel cells depicted in Table 2 (5%-100% hydrogen) operate in a fundamentally very similar way. That is, while the kinetics may slow somewhat at high dilutions of hydrogen in the reactant gas mixture, the operation of the fuel cell is, in essence, the same.

Table 2. Parameters obtained from the Tafel plots: slope A, and the exchange current density i_o. Data from electrochemical impedance: double-layer capacitance within the catalyst layer $C_{(ct)}$, charge transfer resistance $R_{(ct)}$, diffusional resistance Z(d).

H_2 %	A mV/dec	i_o mA/mg_{PtPd}	$R_{(ct)}$ Ω	$C_{(ct)}$ F	$Z_{(d)}$ Ω
100	124	18	0.22	$1.1{\cdot}10^{-4}$	2.67
50	155	32	0.26	$8.9{\cdot}10^{-5}$	2.75
40	169	37	0.26	$8.8{\cdot}10^{-5}$	2.79
30	190	32	0.27	$8.6{\cdot}10^{-5}$	2.85
20	165	22	0.28	$8.4{\cdot}10^{-5}$	3.04
10	160	11	0.28	$8.2{\cdot}10^{-5}$	3.80
5	175	8	0.29	$8.0{\cdot}10^{-5}$	7.11

2.5 Electrochemical Impedance Spectroscopy

To better understand the operation of the cell, electrochemical impedance spectroscopy (EIS) was used to break down the total cell resistance into individual polarization contributions. EIS has proved to be very useful in distinguishing processes with different time constants. The preliminary EIS measurements were taken with symmetrically supplied hydrogen (H_2/H_2) and oxygen (O_2/O_2) at the two electrodes of the cell, to determine the anode and cathode transfer functions at the open circuit potential (Voc). The results were compared with cells operated with either H_2 or O_2 at the same conditions[24] (Figure 5).

In the Nyquist diagram (Figure 5(a)), the higher frequency arc ("*charge transfer*") reflects the combination of effective charge-transfer resistances (Rct) associated with the processes at the electrodes and a double-layer capacitance within the catalyst layer (Cct). The low-frequency part of the spectrum ("*mass transfer*") represents the mass-transport limitations.

The impedance spectra in the higher frequency range were simulated with the equivalent circuit shown in Figure 5(d); the inductance of the wires was not considered.

The charge transfer arc for H_2/H_2 shows, as expected, a lower Rct and higher Cct when compared to cells operated with O_2/O_2 and H_2/O_2. Additionally, from the Bode plot (Figure 5(b)), which provides a clearer depiction of the electrochemical processes in the frequency domain, it can be seen that charge transfer for the H_2/H_2 cell occurs at a higher frequency (≈16 kHz) compared to O_2/O_2 and H_2/O_2 (≈10 kHz). The relaxation time t_0 (eq. 7), which is related to the recovery rate of the steady-state when a perturbation is applied to the system, is then shorter for H_2/H_2 than for O_2/O_2 and H_2/O_2 which again indicates faster kinetics.

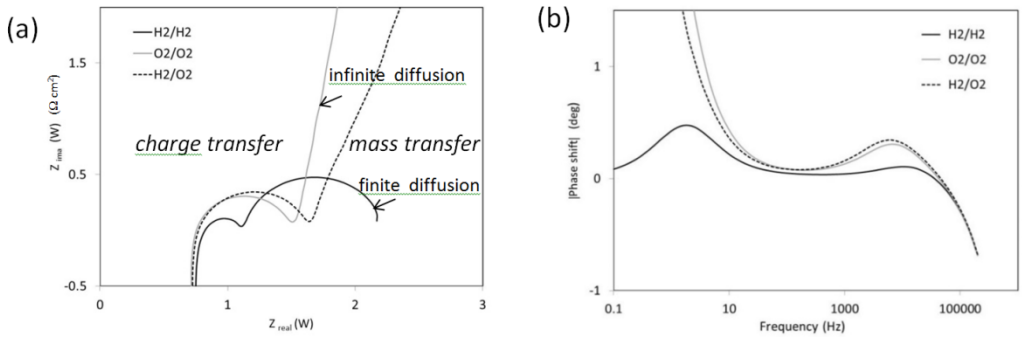

(c)

H_2 %	$R_{(ct)}$ Ω	$C_{(ct)}$ F	i_o mA/mg$_{PdPt}$	t_o ms
H_2/H_2	0.23	8.0E-05	158	0.2
O_2/O_2	0.67	4.0E-05	160	0.3
H_2/O_2	0.76	3.7E-05	172	0.3

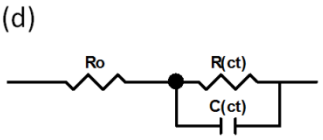

Figure 5. (a) Nyquist and (b) Bode plots of symmetrically supplied hydrogen (H_2/H_2, black line) and oxygen (O_2/O_2, grey line), and unsymmetrically supplied (H_2/O_2, dotted line), at the two electrodes of the cell, at open circuit potential (OCV); (c) table showing charge transfer resistance (Rct), double layer capacitance (Cct), exchange current density (i_o) and relaxation time t_o calculated after fitting the data to equivalent circuit, where R_0 is the ohmic resistance.

$$t_o \approx \frac{1}{\omega_{min}} = \frac{1}{2\pi f} = RC \qquad \text{(eq. 7)}$$

where ω_{min} is the frequency at which the phase shift is minimum.

However the exchange current density i_o, calculated from the charge transfer resistance R_{ct} at open cell voltage (eq. 8), was equal for the anode and cathode: $i_{o\ anode}$ =0.16 A/mg$_{PdPt}$ and $i_{o\ cathode}$ = 0.16 A/mg$_{PdPt}$.

$$R_{ct} = \frac{RT}{zFi_0} \qquad \text{(eq. 8)}$$

where z is the number of electrons involved in overall reaction, R the gas constant, T the temperature and F the faradaic constant. Sheng and co-workers[25] reported somewhat higher numbers (albeit using a 3-electrode system), that were, nevertheless, close for HOR/HER and ORR in 0.1 M KOH and on Pt carbon support ($i_{o\ anode}$=0.35 A/mg$_{pt}$ and $i_{o\ cathode}$ =0.26 A/mg$_{pt}$).[25]

Thus, it can be concluded that the charge transfer resistances of both electrodes contribute significantly to the impedance of the fuel cell (H_2/O_2) at open circuit potential (Voc).

One can also see in the H_2/H_2 case, finite diffusion as an additional loop at the lowest part of the frequency range and infinite diffusion as a straight line with a slopes close to 1 in the O_2/O_2 and H_2/O_2 spectra (Figure 5(a)).

To investigate the EIS of the gas mixtures, spectra were collected at a constant current density of 10 mA/cm^2 (close to the Voc, see Table 1) for: 100%, 50%, 40%, 30%, 20%, 10% and 5% hydrogen in methane mixtures. The results are depicted as Nyquist plots in Figure 6(a). Two arcs are visible for the cell operating with pure hydrogen, which correspond to two relaxation times; namely, the smaller, charge transfer arc at high frequencies (40 kHz-200 Hz) and a larger, mass transfer arc at lower frequencies (200 Hz-0.1 Hz) which describe finite diffusion, also known as the Nernst impedance. To estimate all resistances of the cell from the EIS measurements, the data were fitted to a transmission line model, displayed in Figure 6(b), with the results given in Table 2.

2.6 EIS Data

In general, the intercept of the arc with the real axis at the high-frequency end represents the total ohmic resistance (or electrolyte resistance, often used in fuel cell literature), R_0. The ohmic resistance is recognized to be the sum of the contributions from uncompensated contact resistance and the ohmic resistance of cell components such as electrolyte (electrolyte ionic resistivity) and electrodes.

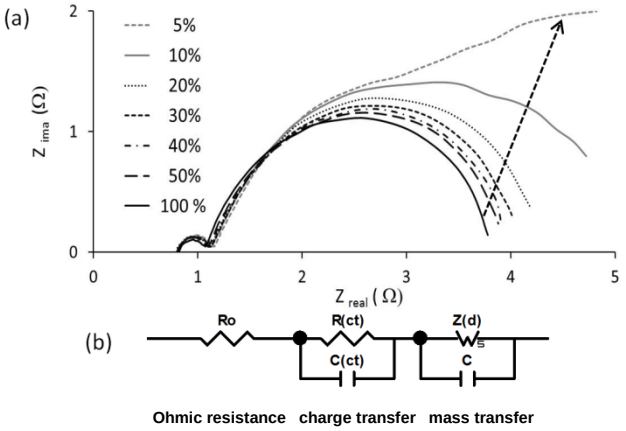

Figure 6. Nyquist spectrum of impedance measurements for cell (1 cm^2) supplied with pure hydrogen and 50%, 40%, 30%, 20%, 10%, and 5% hydrogen and methane mixture. (a) The total flow was kept constant at 20 ml/min, constant current density of 10 mA/cm^2 was applied; (b) the equivalent circuit.

Table 3. Parameters of the flow of H_2 and CH_4 in examined mixtures, and obtained: open circuit voltage (Voc), potential upon applying current density of 10 mA/cm^2, the highest power density (P_{max}) and ohmic resistance (R_{slop_unc}) from uncorrected polarization curves.

H_2 %	H_2 ml/min	CH_4 ml/min	Voc V	E at 10 mA V	P_{max} mW/cm^2	$R_{(i-V)\ slop\_unc}$ Ω
100	1	0	1.04	0.86	44.2	4.0
5	1	19	0.99	0.79	15.4	10.1
4	1	24	0.99	0.77	12.0	12.9
3	1	32	0.98	0.74	9.4	15.8
2	1	49	0.97	0.67-0.59[b]	6.9	20.1
100[a]	1	0	1.02	0.88	36.9	4.8

[a] after methane exposure,[b] within 30 min

For all measured mixtures including pure hydrogen, R_0 remained constant at R_0=0.90±0.01 Ω.

The charge transfer arc varied only slightly with a decrease in the hydrogen proportion within the gas mixture. Thus, the charge transfer resistance changed only from 0.22 Ω cm^2 when using pure hydrogen to 0.29 Ω cm^2 when the hydrogen was diluted to 5% using methane (Table 2). This equates to an ca. 30% increase in the key resistance feature of the cell that essentially determines its overall efficiency. The Gortex-based alkaline fuel cell was clearly highly efficient.

The mass transfer arc of the Gortex-based alkaline fuel cell significantly expanded as the H_2 proportion decreased (Figure 6(a) and Table 2). Increased resistances estimated from this arc indicate longer relaxation times with hydrogen dilution (see. eq. 7), which correspond to a lower freedom of transport within the cell. In common with PEM fuel cells operating with H_2 diluted with inert gases,[2],[12(b)] the mass transfer arc was readily eliminated and the associated mass transfer resistance reduced to zero by simply increasing the overall flow of H_2/inert gas through the anode without changing the diluent proportion.

2.7 Reversibility of the Fuel Cell

After completion of the above measurements with the hydrogen-methane mixtures, the cells were again fed with pure hydrogen and the (j-V) and EIS were compared with the first results obtained using pure hydrogen (Table 1 and Figures 7 (a)-(b)).

The (j-V) results show, that after the cells were exposed to methane, there was a slight increase in the overvoltage at higher current density. Thus, 40 mA/cm^2 less current was generated at the cell voltage of 0.3 V (Figure 7(a)). The maximum power density, which was 109.3 mW/cm^2 (Figure 1(a)), also decreased to 96.7 mW/cm^2 (Figure 7(a)). This may be a result of the reaction being "starved" while collecting the data for 5% and 10%, at higher current densities. However, both (j-V) and (j-P) curves in the range up to 50 mA/cm^2 did not change (Figure 7(a)), indicating that the system was, effectively, fully reversible in this range. That is, the cell essentially recovered its full performance after being treated with the hydrogen-methane mixtures.

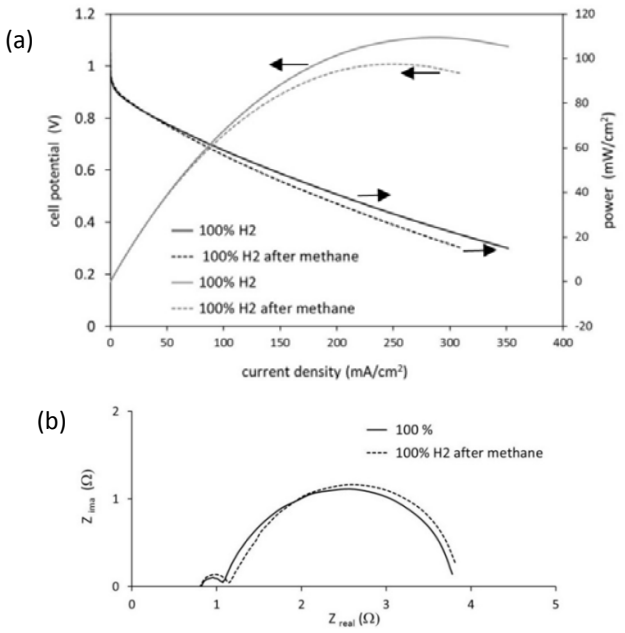

Figure 7. (j-V), j-P) (a) and GEIS at 10 mA/cm^2, (b) characteristics for a fuel cell operating with pure hydrogen before (solid lines, black for j-V and grey for j-P) and after measurements with hydrogen and methane mixtures.

Full reversibility of the cell in the low current density range was also confirmed with EIS performed at 10 mA/cm^2 (Figure 7(b)); the cell demonstrated a fully recovered performance (giving a stable potential of 0.89 V at 10 mA/cm^2, Table 1).

These results are similar to those of Ibeh and co-workers,[2(a)] who used a PEM fuel cell and Pt supported on porous carbon gas diffusion electrodes to extract hydrogen from a mixture with methane. It can be concluded that, methane does not appreciably deactivate the anode catalyst surface under experimental conditions.

2.8 Hydrogen-Methane Mixtures in the Range 2%-5%

To probe lower concentrations of hydrogen in methane, below 5%, a further set of experiments was performed with a fixed flow rate of hydrogen of 1 ml/min in methane (Table 3). In these experiments the cell potential was limited to 0.6 V to avoid cell starvation.

As with the previous set of results, the slopes of the polarization curves (j-V) and (j-P) gradually changed with hydrogen dilution, indicating a further increase in the cell resistances (Table 3 and Figure 8(a)). The potentials monitored at the cell with an applied current density of 10 mA/cm^2, were lower by 70 mV (5%), 90 mV (4%), and 120 mV (3%). All of these were stable. The mixture having 2% hydrogen however (Table 3), originally exhibited a voltage of 0.67 V but after 30 min that gradually changed to 0.59 V which indicated that it was at the border of stability. Galvanostatic EIS measurements at 10 mA/cm^2 also exhibited an increase in resistance deriving from mass transport (Figure 8(b)).

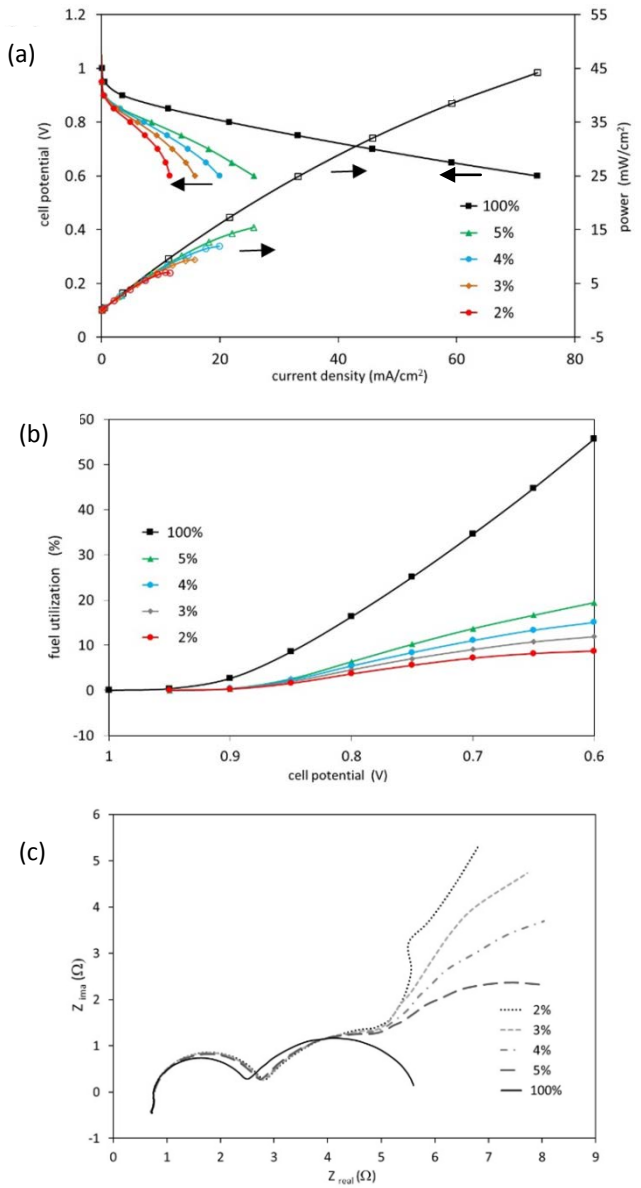

Figure 8. (a) (j-V) and (j-P) characteristics, (b) fuel utilization, and (c) galvanostatic EIS at 10 mA/cm^2 for the cell (1 cm^2) operating with: 100%, 5%, 4%, 3% and 2% hydrogen in the gas mixture.

The extent of fuel utilization (FU) was calculated using eq. 9 and plotted (Figure 8(c)); in all cases the cell was fed with the same amount of hydrogen of 1 ml/min in hydrogen/methane.

$$FU = \frac{Hc}{Hf} * 100 \quad [\%] \qquad \text{(eq. 9)}$$

(where H_c is the theoretically produced hydrogen on the basis of the current intensity and H_f is fed hydrogen). At the low current density of 10 mA/cm^2 (0.8 V), the fuel utilization was $FU_{100\%H2,0.8V}$=16% for the pure hydrogen and $FU_{5\%H2,0.8V}$=6% for the 5% mixture.

As expected for the highest current density at the applied potential of 0.6 V, the difference increased, as did the mass transport resistances. For pure hydrogen, $FU_{100\%H2,0.6V}$ was 56%, whereas for a 5% mixture of hydrogen in methane, $FU_{5\%H2,0.6V}$ was 19%. With further dilution of hydrogen below 5%, the values of FU decreased further.

These results imply that with a more dilute mixture, more hydrogen remains unused. Lower currents generated by the cell with the same amount of fed hydrogen suggest again, that the hydrogen access to the catalyst surface is reduced. However when compared to pure hydrogen, this drop in FU does not follow the percentage of dilution. One of the reasons could be the difference in kinetic diameters, which is quite often invoked in discussing gas permeation in porous materials; these are smaller for hydrogen when compared to methane (2.9 Å vs 3.8 Å).[26]

2.9 Water Balance in the Fuel Cell

While studies did not examine the issue of water balance, it should be noted that water is produced in the Gortex-based fuel cell. Its potential accumulation within the aqueous 6 M KOH electrolyte would therefore need to be considered. The electrolyte is also in direct contact (through the Gortex interface) with the flowing gases, meaning that a humidification equilibrium would be created in the gas chambers. This equilibrium would depend on the operating temperature of the fuel cell and the excess heat it generates. In the process, water vapour from the electrolyte would be taken up by the gases, potentially depleting the water content of the 6 M KOH electrolyte. In a cell fuelled by hydrogen-enriched natural gas, the competing processes of water accumulation and water depletion would ideally be balanced. If that could be achieved, the outlet gas from the anode would contain water vapour and would have to be de-humidified prior to re-entering the natural gas pipeline. In a perfectly balanced system however, the de-humidification step would, effectively, be removing the excess water created during the cell reaction.

3. Conclusions

Utilisation of a novel alkaline fuel cell having Gortex-based gas diffusion electrodes, for power generation from dilute mixtures of hydrogen and methane, has been demonstrated in this work. Mixtures of between 2% and 100% of hydrogen were examined. The following conclusions can be drawn from this study:

1. *Hydrogen dilution:* At a low current density of 10 mA/cm^2, the studied class of AFC can operate efficiently with dilution of hydrogen down to 5% and with an overvoltage of only 60-70 mV above the potential required when the cell is fed with pure hydrogen. Indeed, Tafel plot and EIS studies show that, in terms of the fundamental operation, there is essentially no difference between a 5% hydrogen mixture and 100% hydrogen. In particular, the key measure of charge transfer resistance, which sets the overall efficiency of the cell, displays only an ca.

30% increase in going from pure hydrogen as a fuel, to 5% hydrogen. This seems to be an extraordinary result.

2. *Cell losses:* Mass transport losses, which are dominant in this system, start to appear at low current densities, when the hydrogen concentration goes below 20%. But the increased resistances are only mild down to ca. 5% mixtures of hydrogen. Moreover, they can, effectively, be circumvented by simply increasing the overall flow rate of the dilute hydrogen-methane mix through the cell. The cell can operate successfully under these conditions. At higher current densities depletion of the hydrogen from the mixture becomes a limitation. For a 5% mixture of hydrogen in methane and a flow of 1 ml/min, above potentials of 0.6 V the cell reaction begins to starve, with the highest power density achieved for this mixture being 21.6 mW/cm^2.

3. *Reversibility:* The cells were fully reversible after exposure to methane, which indicates that the methane gas has an inert behaviour in the cell and that no catalyst deactivation occurs.

4. *Gortex electrodes:* The novel Gortex substrates of the electrodes and the aqueous alkaline electrolyte clearly provide a remarkably active solid-liquid interface and ion conductor that allows the fuel cell to selectively extract the hydrogen from the methane and efficiently utilize it as a fuel. These solid-liquid elements are clearly significantly more efficient than the equivalent solid-solid catalyst interface and ion-conductor in PEM fuel cells.

5. *Ability to extract electricity from methane enriched with 5-10% hydrogen:* As natural gas is mostly methane, the present cell offers a potential means of generating electrical power locally by utilizing the dilute 5-10% hydrogen-methane mixtures envisaged for power-to-gas technologies.

4. Experimental Section

Materials: The following materials were employed (Supplier): Carbon black (AkzoNobel), 20% Pt-Pd on Vulcan XC-72 (Premetek Co. # P13A200), Poly(tetrafluoroethylene) (PTFE) (60 wt.% dispersion in alcohols/H_2O; Sigma-Aldrich #665800), KOH 90%, flakes (Sigma-Aldrich #484016), Ni mesh, 200 LPI (Century Woven of Beijing, China) (cleaned using isopropyl alcohol prior to use), and copper tape 6.35 mm width (3M). Polypropylene-backed Preveil^{TM} *expanded PTFE* (ePTFE) membranes with 0.2 μm pore size, produced by General Electric Energy were used in all experiments. Cross-sectional structures were obtained by sectioning and polishing samples fixed in Epo-fix resin (using the cold mounting technique of Struers, Ballerup, Denmark).

Preparation of catalyst-coated Gortex: The catalysts were prepared as a slurry, by weighing out catalyst (20% Pt-Pd on Vulcan XC-7) and carbon black into a 20 mL vial, purging with N_2 for *ca.* 2 min to remove air, then adding isopropyl alcohol (IPA) and water. The mixture was sheared using a homogeniser (IKA T25) with dispersing element (IKA S 25 N – 18 G) at 10,000 rpm for 5 min. PTFE aqueous dispersion was then added dropwise with continuous shearing. After all of the PTFE was added, shearing at 10,000 rpm was continued for another 5 min.

The resulting catalyst slurry was drop-cast onto the Teflon side of the ePTFE membranes (24 mm x 24 mm membrane pieces) and spread out into a square shape measuring *ca.* 12 mm x 12 mm as shown in Figure S1 in the Supplementary Materials. Nickel mesh, which had been laser cut to dimensions 12 mm x 12 mm for the square part with an attached 4 mm x 34 mm neck, was laid on top of the wet slurry and pushed down gently using tweezers to ensure even wetting. Membrane/slurry/mesh assemblies were allowed to dry under ambient conditions.

The dried membrane/slurry/mesh assemblies were compacted using a double-roll mill, having metal rollers. After drying, membrane/slurry/mesh assemblies were rolled three-times through a gap equal to 0.1 mm plus the mesh thickness. For the meshes used, a roller gap of 0.1 mm + 0.15 mm = 0.25 mm was set. As the membrane was ca. 0.2 mm thick, the membrane/slurry/mesh assemblies were compressed by 0.1 mm during rolling.

After rolling, the membrane/slurry/mesh assemblies were weighed. These values were used, together with the weight of the membrane (pre-measured before applying catalyst) and the weight of the mesh (pre-measured before use) to calculate the catalyst loading. The catalyst loading was precisely determined for each electrode; the average was 1.6 g/m^2 metal (Pt/Pd) loading.

Electrode Preparation: Electrodes were prepared by mounting them inside a plastic (PET) laminate that became rigid after passing through a stationery-store laminator. After weighing, each dried and rolled membrane/slurry/mesh assembly was mounted in a pre-cut, folded PET laminate of the type available in stationery stores. The laminate was first cut, using a laser cutter, to a design depicted in Figure S2 (Supplementary Materials), which included a 1 cm x 1 cm window in each side. After folding over, the membrane/catalyst/mesh assembly was placed inside the folded-over laminate such that the membrane / catalyst / mesh was located in the middle of the window (as depicted in Figure S2). The resulting assembly was then fixed in place by carefully passing it through a commercial hot laminator of the type found in stationery stores. In this way, both sides of the catalyst-coated ePTFE membrane remained open and exposed, within the window in the laminate. A small piece of conductive copper tape was attached over the terminus of the neck of the Ni mesh as an electrode contact (see Figure S2).

The 10 mm x 10 mm window in the laminate defined the geometric area of the fuel cell to be 1 cm^2.

Cell Construction: A test cell was custom built to match the dimensions of the laminated electrodes. Figure S3 depicts a photograph and a cross-sectional schematic of such a cell, showing how the laminate-mounted electrodes were placed between the three components of the cell, which were then bolted together using twelve, edge-arrayed screws / bolts. Each laminate-mounted electrode was placed in the cell such that the exposed, windowed catalyst-mesh-coated side faced inwards, toward the facing electrode, and the uncoated back of the ePTFE faced outwards. The cell was assembled using a 3 mm spacer between the electrodes. The gas connections were made using gas-tight fittings. The central cavity of the cell was filled with 6 M KOH.

Reactant Gases and Electrochemical Testing: The hydrogen and methane used in the experiments were stored in high-pressure cylinders connected via suitable polymer tubing to the test fuel cell. In order to obtain the desired mixtures of hydrogen and methane, calibrated mass flow controllers were used (Aalborg, Stanton Scientific, 10 ml/min for H_2 and 50 ml/min for CH_4). The anode compartment of the cell was fed with pure hydrogen or a mixture of hydrogen and methane, while cylinder O_2 gas was supplied to the cathode.

Electrochemical testing was carried out using a Biologic VSP potentiostat. The fuel cells were characterised by steady-state current-voltage (*I-V*) curves, chronoamperometry, and chronopotentiometry. The electrolyte was 6 M KOH. The H_2 (H_2 and CH_4 mixture) electrode (anode) was connected as the working electrode and the O_2 electrode was connected as a combined auxiliary/reference electrode. Thus all reported voltages are *vs.* O_2.

Electrochemical impedance spectroscopy (EIS) measurements were recorded at open circuit or at the constant current density of 10 mA/cm^2 conditions between 0.1 Hz and 200 kHz with an AC amplitude of 10 mV using a potentiostat (Bio-Logic Science Instruments). Spectra were analysed and fitted using ZView version 3.4.

Supporting Information

Supporting information is available from Wiley Online Library or from the author.

Acknowledgements

The authors gratefully acknowledge support under Australian Research Council (ARC) Linkage Grant LP130101135 and from industry partner, AquaHydrex Pty Ltd. PT gratefully acknowledges an ARC Post-Graduate Award (APA). Support from the ARC Centre of Excellence Scheme (Project Number CE140100012) is gratefully acknowledged. The authors acknowledge use of facilities and the assistance of Tony Romeo within the University of Wollongong Electron Microscopy Centre. This research used equipment funded by ARC – Linkage, Infrastructure, Equipment and Facilities (LIEF) grant LE160100063 located at the University of Wollongong Electron Microscopy Centre. The authors thank the Australian National Fabrication Facility (ANFF) Materials Node for equipment use and for design and manufacture of custom-built parts.

Conflicts of Interest

The authors declare no conflict of interest

Keywords

power-to-gas, P2G, alkaline fuel cell, hydrogen, methane

Received:
Revised
Published online:

[1] (a) M. Goetz, J. Lefebvre, F. Moers, A. McDaniel Koch, F. Graf, S. Bajohr, R. Reimert, T. Kolb, *Renewable Energy* **2016**, *85*, 1371; (b) M. W. Melaina, O. Antonia, M. Penev, in "*Blending Hydrogen into Natural Gas Pipeline Networks: A Review of Key Issues*" Technical Report NREL/TP-5600-51995, National Renewable Energy Laboratory, March 2013, and refs therein (https://energy.gov/eere/fuelcells/downloads/blending-hydrogen-natural-gas-pipeline-networks-review-key-issues); (c) "*Power-to-Gas: The Case for Hydrogen - White Paper*", California Hydrogen Business Council, Los Angeles, CA 90049, 2015 and refs therein (https://californiahydrogen.org/sites/default/files/CHBC%20Hydrogen%20Energy%20Storage%20White%20Paper%20FINAL.pdf)

[2] (a) A. Ibeh, *C.* Gardner, M. Ternan *Int. J. Hydrogen Energy* **2007**, *32*, 908; (b) See also studies of contaminant gases in hydrogen feed-gas, for example: X. Cheng, Z. Shi, N. Glass, L. Zhang, J. Zhang, D. Songa, Z.-S. Liu, H. Wang, J. Shen *J. Power Sources* **2007**, *165*, 739, and refs therein; (c) See, Fig. 4 in M. Boillot, C. Bonnet, N. Jatroudakis, P. Carre, S. Didierjean, F. Lapicque *Fuel Cells 06* **2006**, *1*, 31; (d) See, for example: M. T. Dinh Nguyen, S. A. Grigoriev, A. A. Kalinnikov, A. A. Filippov, P. Millet, V. N. Fateev, *J. Appl. Electrochem.* **2011**, *41*, 1033.

[3] M. L. Perry, T. F. Fuller, *J. Electrochem. Soc.* **2002**, *149*, S59.

[4] B. Y. Lin, D. W. Kirk, S. Thorpe, *J. Power Sources* **2006**, *161*, 474.

[5] M. Cifrain, K. V. Kordesch, *J. Power Sources* **2004**, *127*, 234.

[6] A. Tewari, V. Sambhy, M. Urquidi Macdonald, A. Sen, *J. Power Sources* **2006**, *153*, 1.

[7] E. Guelzow, *J. Power Sources* 1996, **61**, 99.

[8] E. Guelzow, M. Schulze, *J. Power Sources* **2004**, *127*, 243.

[9] S. Thyberg, *J. Electrochem. Soc*. **1990**, *137*, 2654.

[10] G. F. McLean, T. Niet, S. Prince-Richard, N. Djilali, *Int. J. Hydrogen Energy* **2002**, *27*, 507.

[11] I. Verhaert, M. De Paepe, G. Mulder, *J. Power Sources* **2009**, *193*, 233.

[12] (a) P. Tiwari, G. Tsekouras, G. F. Swiegers, G. G. Wallace, submitted for publication; (b) K. Wagner, P. Tiwari, G. F. Swiegers, G. G. Wallace, submitted for publication;

[13] B. Winther-Jensen, O. Winther-Jensen, M. Forsyth and D. R. MacFarlane Science **2008**, *321*, 671; B. Winther-Jensen, K. Fraser, C. Ong, M. Forsyth, D. R. MacFarlane *Adv. Mater.* **2010**, *22*, 1727; O. Winther-Jensen, K. Chatjaroenporn, B. Winther-Jensen, D. R. MacFarlane *Int. J. Hydrog. Energy* **2012**, *37*, 8185; B. Kolodziejczyk, O. Winther-Jensen, B. A. Pereira, S. S. Nair, B. Winther-Jensen *J. Appl. Polymer Sci.* **2015**, *132*, 42359

[14] M. Wikol, B. Hartmann, J. Brendle, M. Crane, U. Beuscher, J. Brake, T. Shickel, Chap 23 in *Filtration and Purification in the Biopharmaceutical Industry*, Second Edition (Eds. Maik W. Jornitz and Theodore H. Meltzer), Taylor & Francis, 2007; (ii) F. A. AlMarzooqi, M. R. Bilad, B. Mansoor, H. A. Arafat *J. Mater. Sci.* **2016**, *51*, 2017.

[15] See, for example: Z. Radivojeviz, J. Saunamaeki *International Patent Application WO2009074160A1*.

[16] See, for example: I. Moussallem, J. Jorissen, U. Kunz, S. Pinnow, T. Turek *J. Appl. Electrochem*. **2008**, *38*, 1177, and references therein.

[17] A. F. Gulla, J. L. Krasovic *International Patent application WO2013037902*, and references therein.

[18] A. J. Bard, L. R. Faulkner, *Electrochemical Methods: Fundamentals and Applications*; Masson, 1982.

[19] M. S. Naughton, A. A. Moradia, P. J. A. Kenis, *J. Electrochem. Soc*. **2012**, *159*, B761.

[20] R. J. Gilliam, J. W. Graydon, D. W. Kirk, S. J. Thorpe, *Int. J. Hydrogen Energy* **2007**, *32*, 359.

[21] L. Genies, R. Faure, R. Durand, *Electrochim. Acta* **1998**, *44*, 1317.

[22] T. Shinagawa, A. T. Garcia-Esparza, K. Takanabe, *Sci Rep* **2015**, *5*, 13801.

[23] G. Almutairi, A. Dhir, W. Bujalski, *Fuel Cells (Weinheim, Ger.*) **2014**, *14*, 231.

[24] N. Wagner, W. Schnurnberger, B. Muller, M. Lang, *Electrochim. Acta* **1998**, *43*, 3785.

[25] W. Sheng, H. A. Gasteiger, Y. Shao-Horn, *J. Electrochem. Soc.* **2010**, *157*, B1529.

[26] N. Mehio, S. Dai, D.-E. Jiang, *J. Phys. Chem. A* **2014**, *118*, 1150.

Entry for the Table of Contents

FULL PAPER

Numerous electric and gas utilities are actively pursuing *"Power-to-Gas"* (P2G) technology, which involves using excess renewable power to manufacture hydrogen gas (H_2) that is then injected into the existing natural gas pipeline network in 5-10% by volume. This work reports a novel alkaline fuel cell that may potentially harness such mixtures to generate electrical power. The fuel cell sustainably generates electricity when fuelled with 5% H_2 in methane (CH_4).

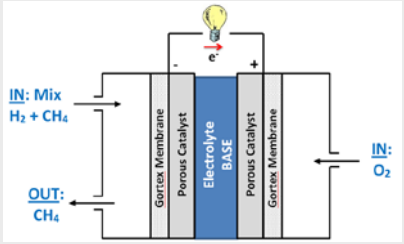

Klaudia Wagner, Prerna Tiwari, Gerhard F. Swiegers* and Gordon G. Wallace*

Page No. – Page No.

Alkaline Fuel Cells with Novel Gortex-based Electrodes are Powered Remarkable Efficiently by Methane Containing 5% Hydrogen